

THE HOST GALAXY OF MARKARIAN 231

DONALD HAMILTON AND WILLIAM C. KEEL¹

National Optical Astronomy Observatories²

Received 1986 October 6; accepted 1987 January 26

ABSTRACT

We present digital images and spectra of the host galaxy of Markarian 231. Its morphology does not fall within standard classification schemes, but suggests a merger or other violent dynamical disturbance. Spectral features from a young stellar population and ionized gas are present, and the stellar population is younger than normally found in high-luminosity galaxies of any type. H II region-like emission is found only in one area; spectroscopic data suggest a sudden, galaxy-wide cutoff in star formation or show a less extreme, but unusually young, stellar population.

A spatially resolved narrow-line region has been identified, of unusually low density and extent ~ 10 kpc. Gas further out in the galaxy is contiguous with this narrow-line region and appears to be ionized by the nuclear continuum (or possible shocks) but is of such low ionization that the extinction on nearly all lines of sight must be comparable to that which we observe; that is, the clouds responsible for reddening the nuclear continuum have a covering factor near unity.

Low-level emission emitted blueward of the prominent disk emission is found to cover a large area and may be related to high velocity outflow of material from the nucleus.

Subject headings: galaxies: individual (Mrk 231) — galaxies: nuclei

I. INTRODUCTION

The active nucleus of Mrk 231 is extreme or unique in many respects. It is most noteworthy for very strong, broad absorption lines blueshifted by as much as 5000 km s^{-1} with respect to the emission-line peaks (Adams and Weedman 1972; Boksenberg *et al.* 1977). Measurements of optical emission-line ratios, continuum shape, and thermal-infrared flux all indicate that very substantial reddening occurs on the line of sight to the nucleus (e.g., Rieke and Low 1972; Cutri, Rieke, and Lebofsky 1984); with the object's high observed luminosity, this implies a total energy output in the range usually associated with quasars. As the only known "broad absorption-line Seyfert," this object may act in some ways as a link with broad absorption-line quasars, and furnish unique information on the geometry and kinematics of dense clouds around a nearby active nucleus (Rudy, Foltz, and Stocke 1985).

A lesser known characteristic of the nucleus, which again bears some resemblance to quasars, is the extreme variability of both the optical (Hamilton and Keel 1987) and the radio flux densities (McCutcheon and Gregory 1978).

The host galaxy of Mrk 231 exhibits its own peculiarities. Direct images, while suggesting spiral structure, show considerable asymmetry (Adams 1977). Its luminosity in the $1.6\text{--}2.2 \mu\text{m}$ range is comparable to that of a giant elliptical galaxy, as are its *JHK* color indices, although the latter are not strong functions of the constituent stellar population (Cutri, Rieke, and Lebofsky 1984). Adams (1972) and Boksenberg *et al.* (1977) have reported a system of high-order Balmer absorption lines, close to the redshift of the emission-line peaks which might be ascribed to stars close to the nucleus; the integrated spectral type of such a population would be near MK spectral type A.

¹ Also Sterrewacht, Leiden.

² The authors have been or are associated with various divisions of NOAO, which is operated by the Association of Universities for Research in Astronomy, Inc., under contract with the National Science Foundation.

Spectroscopy of quasar "nebosity" has suggested that the stellar and gaseous components of their host galaxies may be systematically peculiar (Boroson and Oke 1982; Boroson, Persson, and Oke 1985). Many of them are also morphologically peculiar, with distortions or tails such as result from tidal encounters (e.g., Hutchings *et al.* 1984). Even 3C 273 is not centered in the low-level isophotes of its host galaxy (Tyson, Baum, and Kreidl 1982). At lower luminosities, mergers or interactions seem to play a role in the occurrence of radio galaxies (Heckman *et al.* 1987) and Seyfert nuclei (Dahari 1985; Keel *et al.* 1985). Based on these results, it is of special interest to examine the galaxies around such high-luminosity active nuclei as that of Mrk 231.

This may also serve as a test case for the effects of a violently active nucleus on material in the interstellar medium (hereafter ISM) of its parent galaxy. The absorption-line systems in Mrk 231 show that mass outflow at high velocities and significant column densities is occurring in at least some areas, while the heavy dust shrouding the nucleus will drastically reduce the role of nuclear UV- and X-radiation in creating a wind in the ISM (Begelman 1985). This could serve as an unusually pure tracer of the kinetic-energy influence of a violently active nucleus, with minimal confusion from radiatively induced phenomena.

To define the properties of the galaxy more closely and examine any relationship between its peculiarities and the active nucleus, we have obtained new, high-quality images and spectra. We present them here, with some implications for the history of the galaxy and physical condition near the nucleus.

II. OBSERVATIONS

a) Images

A set of images in *B*, *V*, *R*, and a narrow passband including H α (defined by an interference filter with peak transmission at 6826 \AA and half-power width 82 \AA) was obtained on 1985 May

TABLE 1
CCD PHOTOMETRY

Aperture	V	$B-V$	$(V-R)_{\text{KC}}$
6"0	13.43	0.75	0.52
30.0	12.97	0.68	0.51
12.8, disk	15.20	0.46	0.51
15.0, disk	15.04	0.46	0.51
20.0, disk	14.77	0.46	0.51
30.0, disk	14.12	0.56	0.50

NOTES.—KC refers to the Kron-Cousins system. Disk refers to nucleus removed (6" aperture), and replaced with an equal area of same surface brightness as in the 6"-12"8 annulus.

22 using an 800×800 TI CCD at the Ritchey-Chrétien focus of the KPNO 2.1 m telescope; each pixel covers $0''.20$ on a side. The seeing was excellent, with a FWHM for stellar images of $1''.2$ measured on the frames. The image quality was limited by the stability and alignment of the telescope optics, rather than the seeing. Photometric calibration was performed through observation of a "standard" field in M92 (Christian *et al.* 1985) and assuming mean extinction coefficients. Moderate moonlight was present, so the contrast of very faint structures was reduced.

The images in all passbands appear very similar; they are shown in Figure 1 (Plate 1), with various gray scales to emphasize structures over a wide dynamic range. Structures of interest are present at almost every surface-brightness level. These will be discussed in § III.

The precise photometric scale of our CCD is important, since we use these data to derive colors and magnitudes for the galaxy without the nuclear contribution. An external check has been performed, comparing synthetic-aperture photometry from the CCD frames (Table 1) to photoelectric aperture photometry (Table 2). Data are available from Weedman (1971), and measurements we have obtained in 1980 and in 1984 at Lick (0.9 m Crossley reflector) and Mount Lemmon (1.5 m) Observatories. These latter observations were transformed to the Johnson system (the filter and photomultiplier used at Mount Lemmon were designed to match the Johnson *UBVRI* system). The 1980 and 1984 measurements agree well with each other, but not with the 1971 data. Because of the likelihood of a photometric outburst in the interim, we compare (Table 1) CCD aperture photometry to these data (Table 2). The agreement is close enough (especially in the presence of a variable nucleus) that our photometric scale is confirmed. Also in Table 1, we give magnitudes and color indices estimated from the

TABLE 3
ANNULAR COLOR INDICES

Annulus	$B-V$	$(V-R)_{\text{KC}}$
10"-20"	0.49	0.61
20-30	0.18	0.77
30-40	-0.09	0.98
40-50	-0.22	0.74

NOTE.—Because of the range of standard $B-V$ color indices observed, the transformation equations become an extrapolation for very blue indices.

"disk" of Mrk 231 excluding the nucleus. The galaxy (less nucleus) is quite luminous in the optical range, $M_B = -22.5$, as it is in the infrared (Cutri, Rieke, and Lebofsky 1984), but has such a large linear scale that the surface brightness is rather low. Its blue colors accord with spectroscopic information on its stellar composition (§ IV). Table 2 includes, in addition, data on three giant elliptical galaxies, for comparison. Boksenberg *et al.* (1977) suggested that the slope of the nuclear continuum of Mrk 231 between 6000 and 10000 Å to be greater than that of a nearby giant elliptical galaxy. We find, however, that Mrk 231 is bluer in all color indices than the old populations found in giant elliptical galaxies, despite its strongly reddened nuclear continuum.

We performed synthetic annular photometry from the CCD images. The results, given in Table 3, demonstrate the existence of significant color gradients in $B-V$ and mild gradients in $V-R$. The bluing effect at larger annuli is consistent with a merging system where star formation is proceeding in the outer regions. No obvious foreground stars contributed to the annular photometry.

Inspection of the B , V , R , and $H\alpha$ images presented in Figure 1 hints that the primary contribution to the $H\alpha + [\text{N II}]$ bandpass is continuum radiation. Subtraction of the $H\alpha$ and R images, after appropriate renormalization, reveals a low-level, diffuse, and widespread $H\alpha/[\text{N II}]$ emission. The resultant image, presented in Figure 2 (Plate 2), shows the diffuse halo, blending into the "horseshoe" south of the nucleus (discussed further below) and what appears to be two spiral-arm-like features.

The H II region-like spectra we found are coincident with the bright enhancement $\sim 12''$ south of the nucleus seen in Figure 2. This enhancement might be an extension of a narrow tidal feature or even possibly of a spiral arm.

TABLE 2
PHOTOELECTRIC PHOTOMETRY

Object	V	$U-B$	$B-V$	$(V-R)_J$	$(R-I)_J$	Aperture/Telescope
M231	13.36	0.00	0.74	0.73	0.45	12"8/ML60
M231	13.22	0.00	0.72	20. /MH36
NGC 4889	14.24	0.48	1.03	0.91	0.62	12.8/ML60
NGC 4839	14.53	0.54	0.97	1.05	0.66	12.8/ML60
NGC 4472	11.94	0.69	0.92	0.92	0.77	12.8/ML60

NOTES.—Previous photoelectric measures from Weedman 1971: $V = 13.84$, $B-V = 0.84$, $U-B = +0.15$ within 15" aperture. Assuming $A_V = 0.21$ mag for M231; $A_V = 0.15$ for giant elliptical galaxies; ML60 = Mount Lemmon 60-inch telescope plus VPM 159; MH36 = Lick Crossley telescope plus FW 130. Observations with ML60 on 1984 May 26 and 27; those with MH36 on 1980 March 20. Photometric precision for the ML60 photometry is 2%, 3%, 3%, 4%, 4% in V , $U-B$, $B-V$, $(V-R)_J$, $(R-I)_J$, respectively.

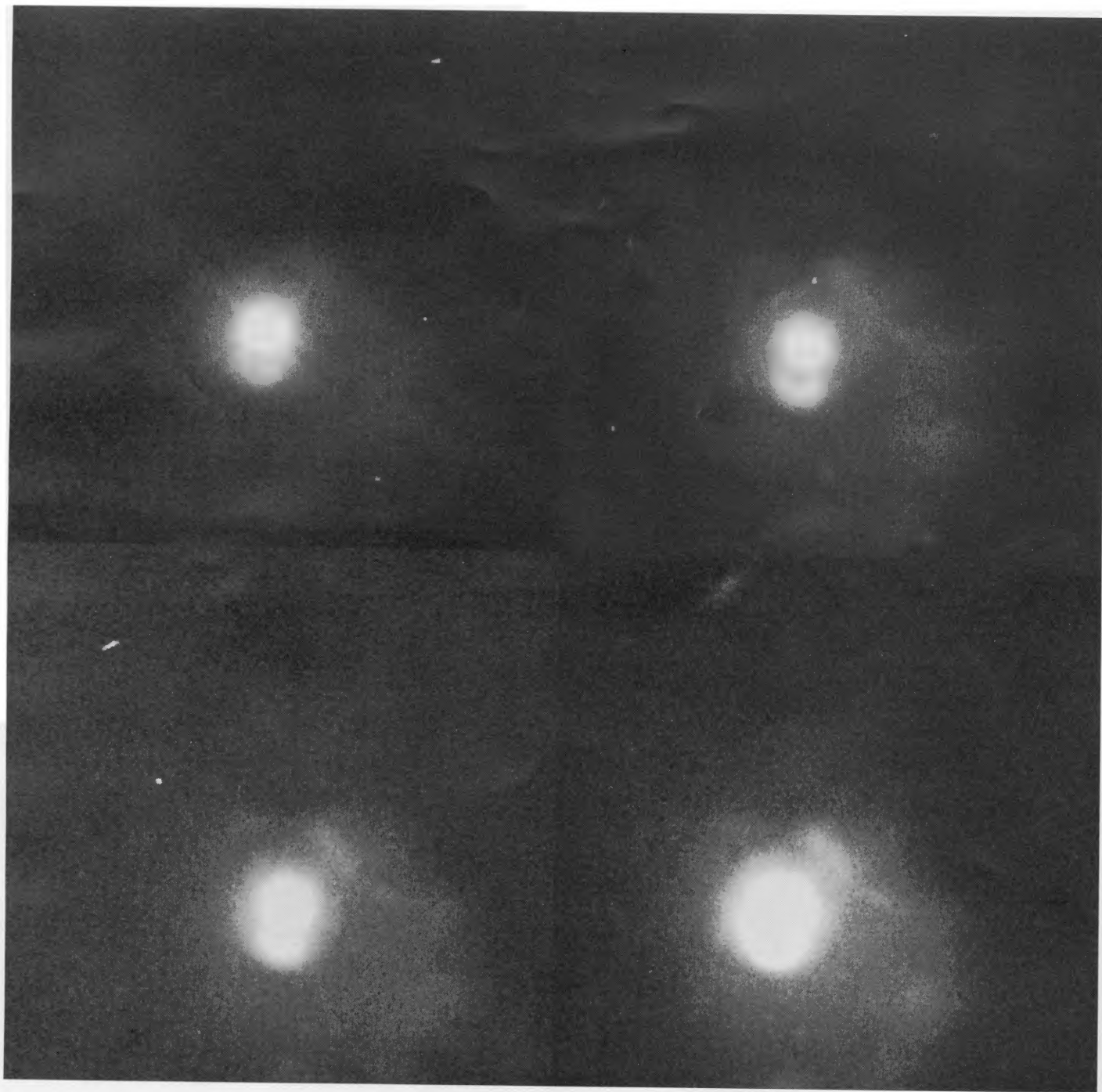


FIG. 1.—*B* (lower right), *V* (lower left), *R* (upper right), and $H\alpha$ (75 Å wide centered at 6825 Å; upper left) images obtained with a TI CCD on the Kitt Peak 84 inch telescope. Exposure times were 8, 3, 3, and 15 minutes, respectively. Note the diffraction spikes from the nucleus. South is to the bottom, and west is to the right. Each image is $\sim 48''$ on a side.

HAMILTON AND KEEL (see 321, 212)

PLATE 2

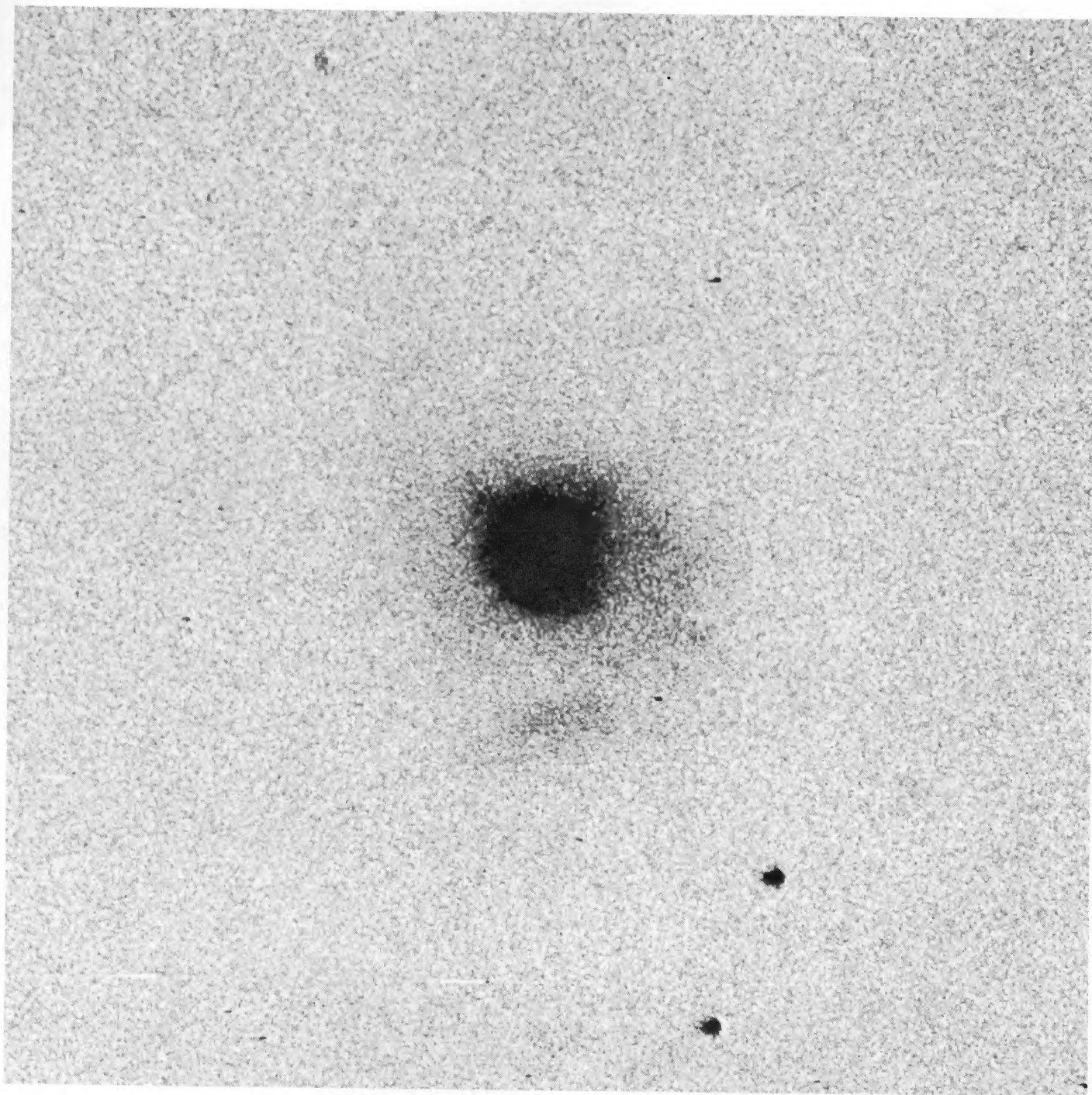


FIG. 2.— $H\alpha$ plus $[N\ II]$ image of the galaxy. South is to the bottom, and west is to the right. The image is $\sim 98''$ on a side.

HAMILTON AND KEEL (see 321, 212)

TABLE 4
JOURNAL OF SPECTROSCOPIC OBSERVATIONS

Telescope	Date (UT)	Detector	Exposure (minutes)	Wavelength Range	Resolution (Å)	P.A.	Offset	Slit Width	Remarks
KPNO 4 m	1984 Dec 21	CC	20	4500–7900	15	90°	0"	2.5	Clouds
KPNO 4 m	1985 Jul 4	TI	30	6520–7040	5.5	158	0	1.7	
KPNO 4 m	1986 Feb 28	CC	15	6000–9000	15	0	0	2.5	
KPNO 4 m	1986 Feb 28	CC	20	6000–9000	15	0	2.7 W	2.5	
KPNO 4 m	1986 Feb 28	CC	16	6000–9000	15	0	5 W	2.5	
KPNO 4 m	1986 Mar 2	CC	10	6000–9000	15	90	0	2.5	Clouds
KPNO 4 m	1986 Mar 2	CC	60	6000–9000	15	90	4.5	2.5	Clouds
INT 2.5 m	1985 Dec 19	IPCS	43	4750–5700	0.9	90	4.5	1.0	
INT 2.5 m	1985 Dec 19	IPCS	20	4750–5700	0.9	90	0	1.0	

NOTES.—Detectors: CC = Cryogenic Camera with TI CCD. Pixels 4.25 Å by 0".84; TI = Ritchey-Chrétien spectrograph with No. 2 TI 800 × 800 CCD, pixel size 0.65 Å by 0".31; IPCS = image photon-counting system on intermediate-dispersion spectrograph at Isaac Newton telescope, pixel size 0.46 Å by 0".63.

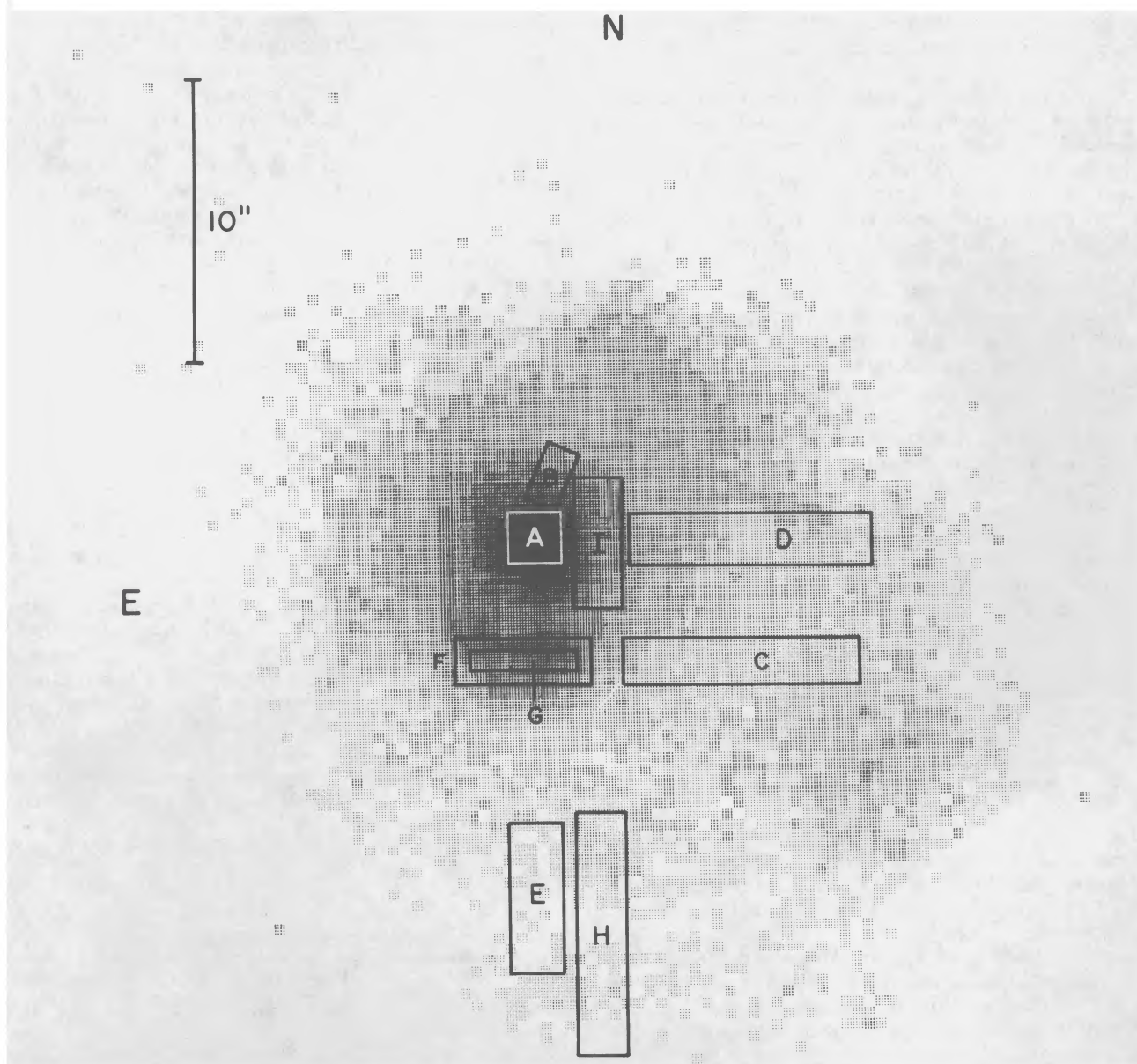


FIG. 3.—Schematic of the bright central regions. The apertures from which the spectra were extracted are outlined with bold lines. The label of the box is the same as the label of the spectrum presented in Fig. 4.

b) Spectra

We have obtained spectra at a variety of dispersions covering several parts of the host galaxy of Mrk 231. The wavelength ranges and positions observed are given in Table 4. The low-dispersion Cryogenic Camera data were placed on an absolute ($\pm 5\%$) flux scale through observations of Oke and Gunn (1983) standard stars, all observed through a $10''.8$ wide slit under absolutely photometric conditions. Standard extinction values for Kitt Peak were assumed, and all Cryogenic Camera reductions were performed using IRAF.

We attempted to use a set of slit positions that sample most important regions of the galaxy as seen in the direct images: the "horseshoe," the bright "rim" northwest of the nucleus, the extensive plateau on the west side of the galaxy, and fair coverage of the area immediately surrounding the nucleus. This is shown in Figure 3, in which the slit locations (reduced to that spatial part used in the summed spectra) are superposed on a representation of the inner part of Mrk 231. Several areas for which spectra have been extracted for analysis are indicated.

Spectra of some of the areas marked in Figure 3 are presented in Figure 4. The nuclear spectrum (Fig. 4a) has been discussed extensively elsewhere (e.g., Boksenberg *et al.* 1977), and we will have relatively little to add. The Appendix is a brief discussion of our analysis of the nuclear spectrum. A weak narrow-line region (NLR) is present in $H\alpha$, $[N II]$, and $[S II]$ (Fig. 4b), which blends into similarly low-ionization emission extending across most of the face of the galaxy (Fig. 4c). Stellar absorption features are present in at least the "plateau" region (Fig. 4d). Effects of recent star formation are seen in the southern "rim," in the form of $H II$ region emission lines (Fig. 4e). The strongest and highest ionization emission is seen in the "horseshoe," with not only $H\alpha + [N II]$ (Fig. 4f) but also double-peaked $[O III] \lambda 5007$ (Fig. 4g).

Emission features have been measured, using Gaussian fits to deblend lines and estimate widths. The results are discussed in § Vc. Absorption lines ($H\beta$ and the $Mg b$ band) were measured in the plateau spectra (§ IV). $Na D$ absorption was detected in several places. Comparison of data from different nights suggest that continuum shapes (from Cryogenic Camera data) are reliable to $\sim 5\%$ over a 3000 \AA interval.

III. GALAXY MORPHOLOGY

As is evident from the images in Figure 1, the galaxy of Mrk 231 does not fall within any of the usual galaxy classification schemes. On the basis of lower quality images, it has occasionally been considered as some kind of peculiar Sc system, but we find this classification unsatisfactory for several reasons:

1. The features which might be identified as spiral arms are very uneven in pitch angle and width.
2. The southwest "arm" is very broad, with none of the small-scale absorption or narrow ridges usually associated with spiral features.
3. No giant $H II$ regions appear along the putative arms, which is unheard of among late-type spirals; however, one $H II$ region, not associated with the obvious "arms," may be present from the examination of Figure 2, $\sim 12''$ south of the nucleus.
4. No clear disk (quasi-exponential) component can be fitted to the surface-brightness distributions in a two-

dimensional sense. Residual structures of comparable spatial scale are much brighter than such a disk component could be.

5. The northern arm-like extension is more likely a tidal tail. This interpretation is supported by the presence of an opposing feature at lower surface brightness, as shown in Figure 5 (Plate 3). This image is a registered stack of B, V, R data binned 2×2 from the original data, and smoothed with a $1''.2$ running box to show very faint structures.

The twin-tail appearance of the system on deep images strongly suggests that this is the aftermath of a galaxy merger, while the asymmetric inner light distribution argues that the greatest disturbance must have taken place only a few dynamical times ago. Under these circumstances, the lack of coherent structure is hardly surprising, as in the Antennae, NGC 4038/4039 (Burbidge and Burbidge 1966). The azimuthally averaged surface brightness profile of such a system approaches an equilibrium state much more quickly than the projected intensity distribution itself; however, Schweizer (1982) found the "wreck" NGC 7252 to approximate an $r^{1/4}$ law, using aperture photometry to derive average surface brightness data. Similar treatment of the Mrk 231 R -image (Fig. 6) shows that the azimuthally averaged profile might be fitted by either the $r^{1/4}$ distribution that approximately fits the profiles of some elliptical galaxies or the exponential form used empirically for spiral disks. Examination of the images themselves shows that neither "fit" has any particular physical significance, although the resemblance of the "curves of growth" in the near-infrared led Cutri, Rieke, and Lebofsky (1984) to propose that Mrk 231 is a giant elliptical galaxy—the one classification that we can definitely rule out from the images.

White (1978) noted, based on his N -body simulation, that the profile of the galaxy that results from a merger, could mimic an $r^{1/4}$ form. Another conclusion based on White's analysis was that whenever the impact parameter is small, the resultant galaxy has a higher central concentration and a more extensive envelope than either progenitor galaxy. The optical appearance of Mrk 231 conforms in this respect with White's resultant theoretical galaxy.

Crude BVR photometry was performed on the tails themselves, and on the amorphous luminous material northeast of the galaxy (see Fig. 5). Strips (E-W for the tails, N-S for the NE region) were summed across the BVR images, avoiding the galaxy envelope as far as possible and nearly normal to the tail orientation. The mean colors and surface brightnesses of the regions as measured are given in Table 5. The color indices of both tails and the amorphous material are all similar and blue by galaxy standards, $B - V \sim 0.4$ and $(V - R)_{KC} \sim 0.6$. These colors, which are similar to those found in the disk (see Table 1), are characteristic of an intermediate-age population, which is perhaps to be expected since star formation has been proceeding vigorously across the galaxy for ~ 2 Gyr (§ IV). Star formation does occur in tidal tails themselves, not only in the

TABLE 5
SURFACE BRIGHTNESS OF FILAMENTS

Area	SB_B	SB_V	SB_R	$B - V$	$(V - R)_{KC}$
NE	25.78	25.38	24.36	0.40	1.02
N tail	24.70	24.28	23.64	0.40	0.64
S tail	25.43	24.84	24.11	0.59	0.73
Sky ^a	22.51	21.50	21.11	1.01	0.39

^a Moon was 3–4 days from zero phase.

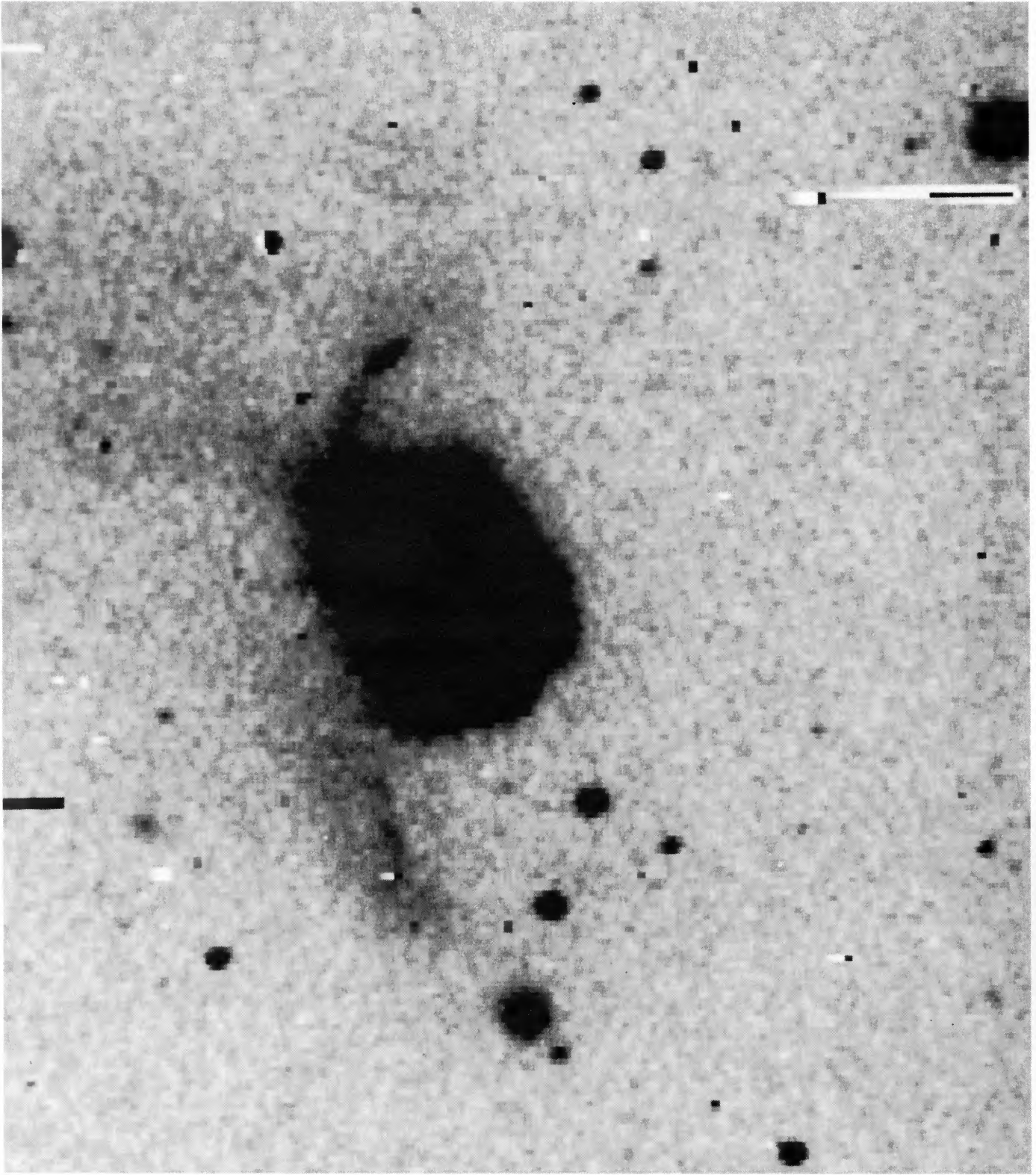


FIG. 5.—Coadded image of B , V , and R binned two pixels to one, and smoothed by a $1\frac{1}{2}$ running box. Note the tidal tails and the amorphous faint nebulosity to the northeast. South is to the bottom, and west is to the right, and the image is $\sim 138''$ on a side.

HAMILTON AND KEEL (*see* 321, 214)

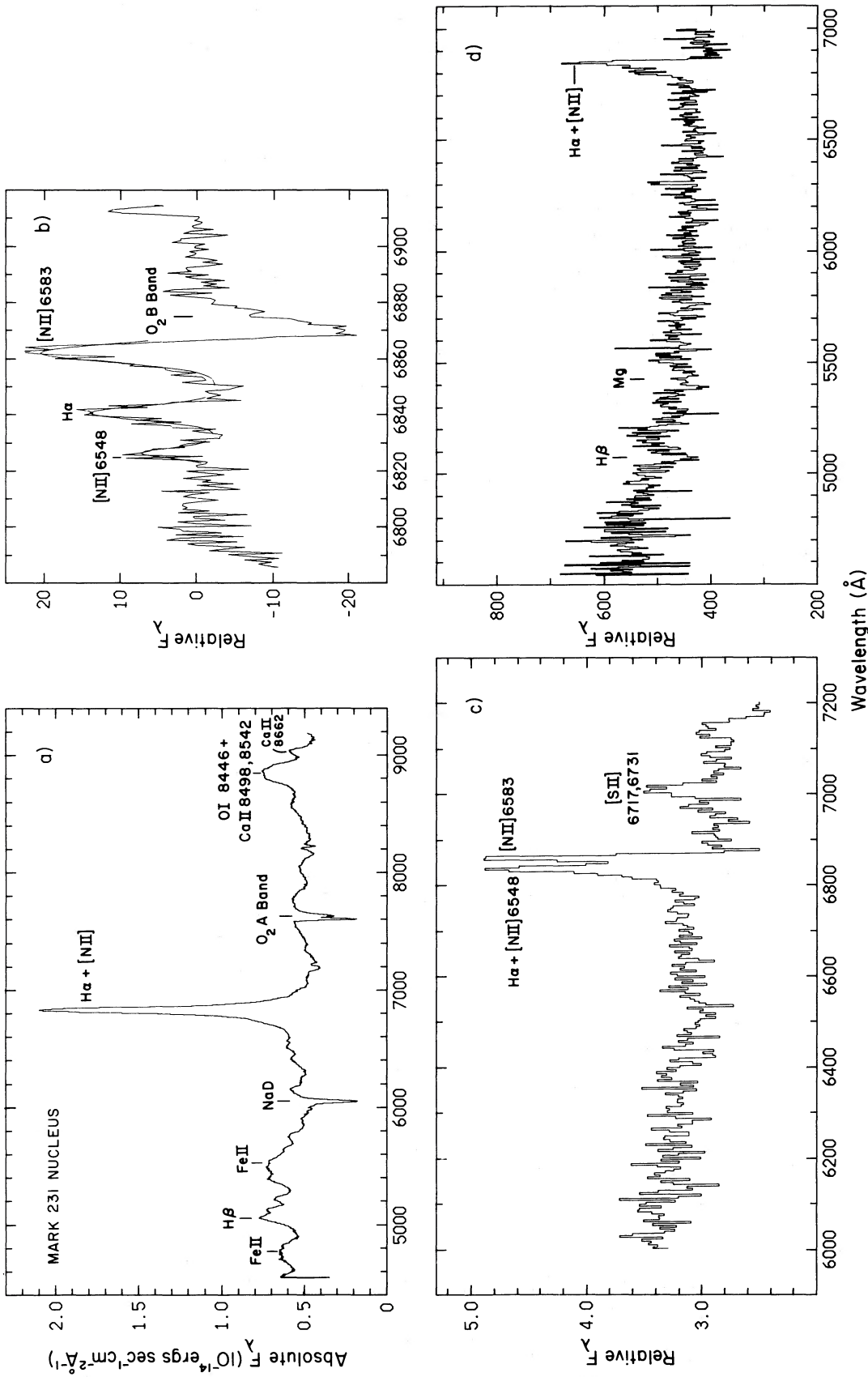


FIG. 4.—(a) Merged nuclear spectrum of Mrk 231 from Cryogenic Camera data of 1984 December (blue) and of 1986 February (red). The spectrum of 1984 December was scaled to the spectrum of 1986 February which was taken in absolutely photometric conditions. (b) A spectrum of the narrow-line region found to be in or near the nucleus and obtained with the 4 m RC spectrograph plus TI CCD. Curves are Gaussian approximations. A correction for scattered nuclear (broad-line) light has been applied. As in Fig. 3, this area is $\sim 2''$ off the nucleus. (c) Spectrum of the low ionization emission found in the disk of the galaxy. (d) Spectrum of the nebulosity found toward the west of the nucleus. Note the existence of H β and Mg *b* absorption features. (e) Spectrum of the region found at $10''$ – $15''$ south of the nucleus. The spectrum resembles that of an H II region. (f) Spectrum of the bright region $\sim 4''$ south of the nucleus. The area, because of its shape, is referred to as the “horseshoe.” (g) A spectrum of the horseshoe region obtained with the IPCS showing double [O III] $\lambda 5007$ emission.

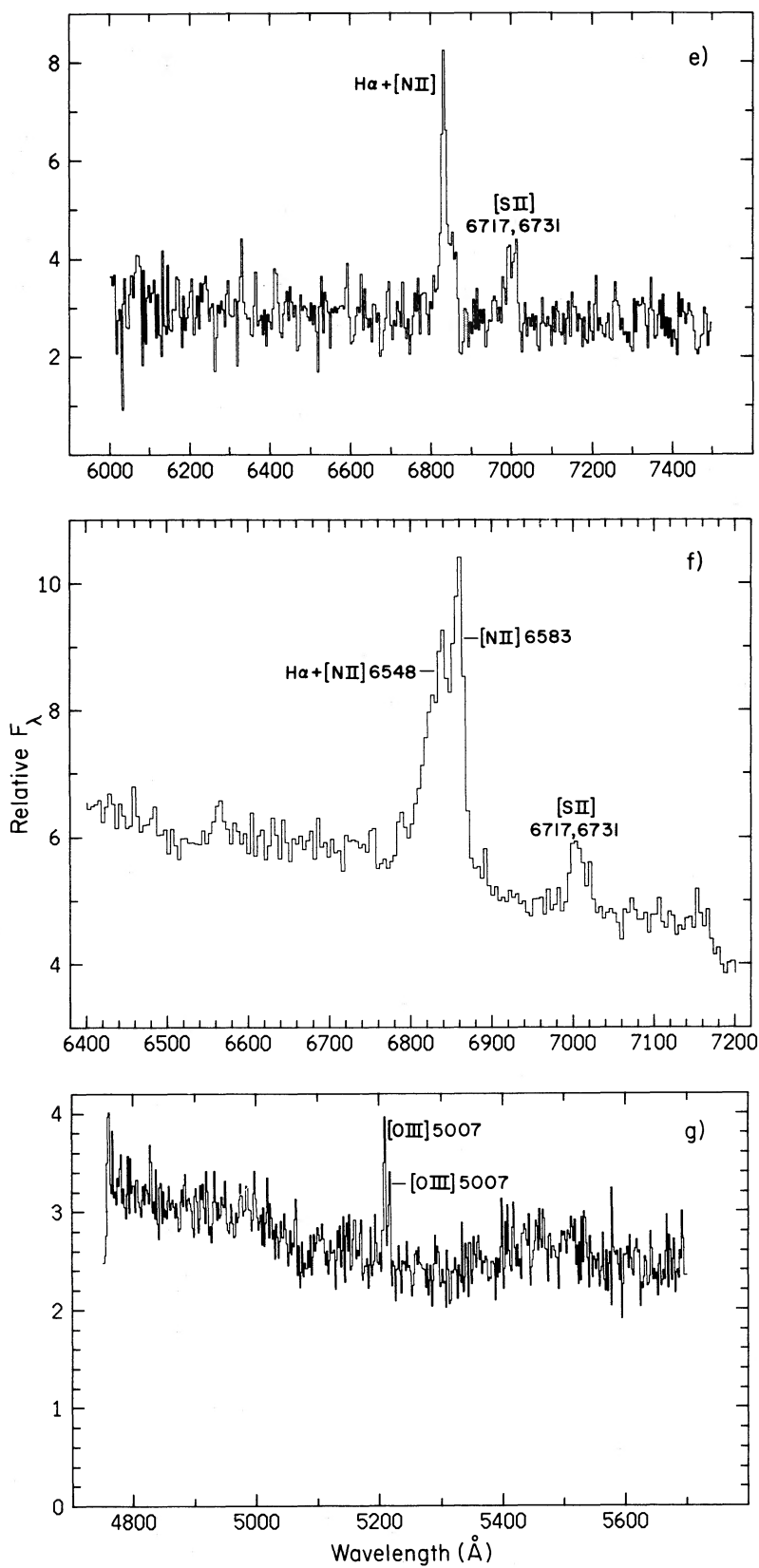


FIG. 4—Continued

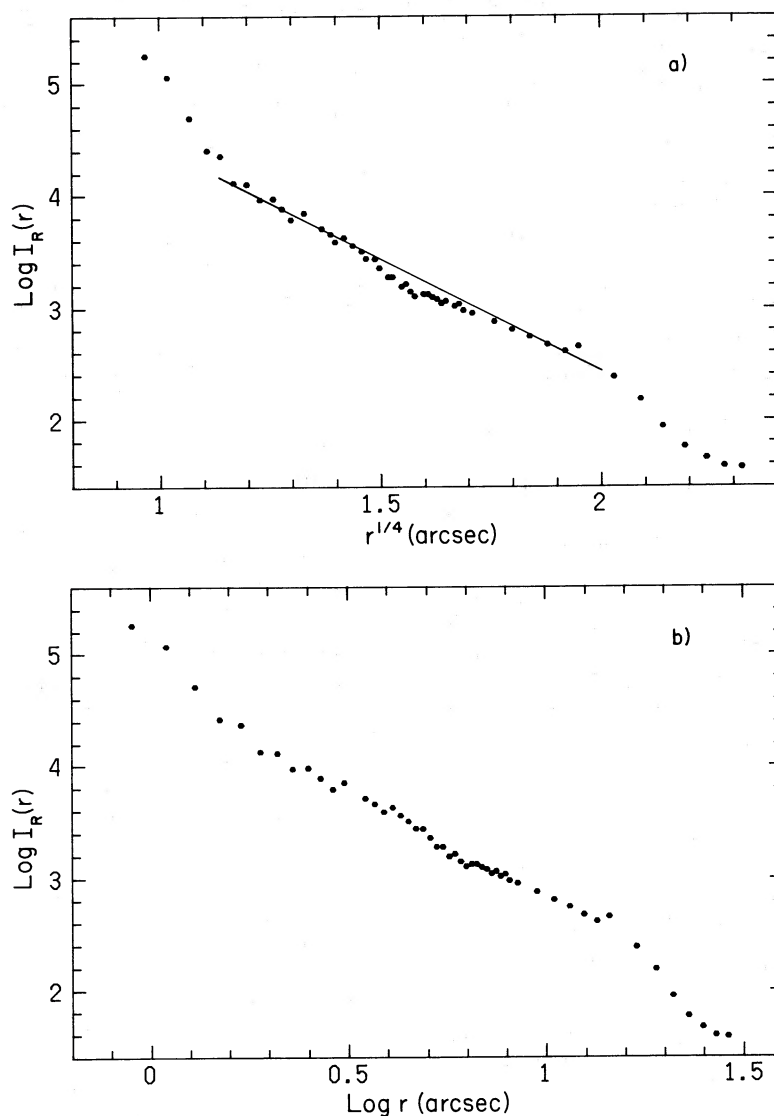


FIG. 6.—(a) Azimuthally averaged profile from the R CCD image and plotted against $r^{1/4}$. A straight line is drawn through the middle portion to indicate the significance of the fit. (b) Same as (a), but for $\log r$ along the abscissa.

disks, as seen by the presence of H II regions in the tails of NGC 4038/4039 (Schweizer 1978). The $(V-R)_{\text{KC}}$ color index differs among the features, with the brightest north tail being bluer; this might reflect different star-forming histories or contributions from an old population.

IV. STELLAR POPULATION

a) Aging Burst versus Truncated IMF

The blue continuum and relatively strong H β absorption both suggest substantial recent star formation across the galaxy. Its light (as seen in the “plateau” spectrum) is dominated by stars of spectral type whose main-sequence ages are of order 1 Gyr. The high luminosity of the ensemble ($M_B \sim -22.5$ for the galaxy less nucleus) indicates that star formation has been very extensive, involving an enormous mass of gas.

The emission lines observed in two areas (Fig. 3, positions H

and E, and the corresponding spectra of Fig. 4) are characteristic of H II region emission, indicating the presence of large numbers of O stars in one region of the galaxy. The rest of the system does not show such emission-line ratios but does exhibit spectral features indicating less recent widespread star formation. This is illustrated by the region west of the nucleus (Fig. 4d). Absorption at H β is clearly present, as is Mg (Table 6).

The continuum shape and absorption-line strengths are consistent with a stellar population of age ~ 2 Gyr, having an effective main-sequence turnoff at $\sim F5$. Their concordance also suggests that reddening of this part of the system is not significant.

In addition to the current star formation directly betrayed by the detection of H II regions, spectroscopic observations of other parts of the galaxy are suggestive of an aging burst population. Limits on H α emission from putative H II regions in the

TABLE 6
SPECTRAL FEATURES 5"–15" WEST OF THE MRK 231 NUCLEUS

Feature	Line	W_λ (Å)
Absorption	H β	4.6 ± 1.0
	Mg <i>b</i> λ 5175	1.3 ± 0.4
	Mg H λ 5200	1.8 ± 0.4
Emission	H α	7.0 ± 1.0
	[N II] λ 6583	$19. \pm 2.0$

other regions (where the intermediate-age population dominates the spectrum) may serve to add constraints on the galaxy's star-forming history. These constraints may be expressed in terms of maximum stellar mass, minimum burst age, or ratio of present to past star-formation rate.

The H α emission actually observed spectroscopically is mostly produced by processes other than stellar photoionization (§ IV) at most points in the galaxy; consideration of astrophysically viable line ratios in comparison with those observed suggests that no more than one-half of the observed H α intensity might be due to normal H II regions. The equivalent width of the part of H α produced by radiated stellar UV continuum must, therefore, be less than 3 Å. Consider a simple two-component population, a young (H II region) population containing OB stars and producing H α , through photoionization and recombination, and an older population in which H α appears in absorption with an equivalent width ϵ . The hot population in this case will contribute at most $(3 \text{ Å} + \epsilon)/W_0$ of the continuum at H α , where W_0 is the H α emission equivalent width of a pure "newborn" population. This quantity is sensitive to the shape of the high-mass portion of the initial mass function and the time scale of star formation (Kennicutt 1983) but is observed to be as high as 100 Å in whole galaxies (Kennicutt 1983) which are not single populations, and 300 Å in individual giant H II regions scaling from the H β results of McCall, Rybski, and Shields (1985). The higher value is more appropriate for this calculation, since it is not strongly influenced by an underlying older population. The H α absorption correction (from stellar atmospheres) varies with the type of older population. Using the synthetic population spectra presented by Keel (1983) and summarized in Table 7, the equivalent width of H α ranges from 1.8 Å for an old (elliptical galaxy) population, to 5.1 Å in the Gunn, Stryker and Tinsley (1981) young (constant SFR) sequence. The latter is closer to what we

TABLE 7
EQUIVALENT WIDTHS FOR KEEL SYNTHETIC POPULATIONS

Population	H β (Å)	Mg I (Å)	Na D (Å)	H α (Å)
MS $T_0 = 15$	3.18 ^a	4.32	4.18	2.02
MS $T_0 = 5$	2.73	3.25	2.02	3.18
MS $T_0 = 1$	8.31	1.55	1.22	4.74
New MS	3.51	...	1.74	3.99
GST Young	8.25	1.06	1.01	5.09
G0 + G5 III	2.78	2.04	1.22	2.84
K0 III	2.56 ^a	3.30	2.53	1.64
K5 III	7.38	5.23	2.05
N3379	3.78 ^a	4.98	5.82	1.65
N4472	3.87 ^a	6.24	4.99	1.0
M32	3.19	3.49	2.99	2.53

^a These measures will be contaminated by the presence of Fe.

believe to be appropriate here, since the continuum shape does not allow a significant contribution from a conventional old population. Adopting $\epsilon = 4 \text{ Å}$, we find that the new population contributes less than 2.3% of the red continuum flux.

This limit may be translated into a value of current SFR in terms of its average over the lifetime of the dominant stellar type in the spectrum, $\sim 2 \text{ Gyr}$. This ratio is approximated by the ratio at $(M/L_R)t_{\text{MS}}^{-1}$ for the two populations; this approach gives a current limit on SFR, that it is no higher than its average over the last 2 Gyr (unless, OB stars are under-represented by comparison with, say, a Salpeter IMF.)

Thus much of the galaxy seems to have undergone a burst of star formation which from our spectroscopic evidence appears to be dying away. Similar blue populations without strong emission lines are rather rare among luminous galaxies; the central regions of the interacting dwarf NGC 4485 show strong Balmer absorption and a blue continuum (Keel *et al.* 1985), while a few Markarian galaxies have similar properties in their inner region (Keel 1987). An especially interesting comparison is possible with the blue absorption-line spectrum of the nebula around 3C 48 (Boroson and Oke 1982). This comparison is discussed in § VI.

Additional information on the star formation history is available from detection of strong CO emission (Sanders *et al.* 1987) corresponding to a molecular hydrogen mass of $\sim 15 \times 10^9 M_\odot$. Thus substantial molecular gas is available for star formation, which might be unexpected if star formation has in fact ceased in most places. The molecular gas/atomic gas ratios may be peculiar; Heckman, Balick, and Sullivan (1978) find $M(\text{H I}) \lesssim 20 \times 10^9 M_\odot$, giving an unusually low $M(\text{H I})/L_B \lesssim 0.09$ (solar units) for the galaxy. This implies that a period of enhanced star formation, or at least H I depletion, has occurred.

These conclusions might be modified by a substantial dilution of light by an old population or by effects of dust absorption. As noted above, little old population contribution is allowed by the lack of Na D absorption and from the shape of the blue continuum; less than $\sim 20\%$ of the light could conceivably come from an elliptical galaxy-like component. Effects of dust are more difficult to evaluate, since its distribution is essentially unknown. A large fraction of the star formation could, in principle, proceed within dense clouds, having virtually no effect on the optical spectrum until the stars escape the clouds, at a rather evolved state. However, such a process has yet to be demonstrated even in the denser environment of a galactic nucleus.

b) Observations in Comparison with Evolutionary Models

It is not possible, with any certainty, to specify the star formation history of a galaxy uniquely since the observations are a result of a product of an initial mass function, age, and star-formation rate. Although the usual parameterization of evolutionary models (see, e.g., Hamilton 1985) uses separable functions (for IMF, SFR etc.); realistically, such a separation is not possible.

To match the observed H β or Mg *b* line indices (to within one standard deviation) with those of the evolutionary models of Hamilton (1985) requires a young population (1–2 Gyr) and a power-law IMF with an exponent of at least 2. (Salpeter IMF exponent is 1.35.) This exponent implies a paucity of high-mass stars relative to that of the solar neighborhood. The strength of the synthetic line indices are more sensitive to the IMF expo-

TABLE 8
SYNTHETIC LINE INDICES

τ (Gyr)	Age (Gyr)	H β (Å)	Mg <i>b</i> (Å)	<i>x</i>
0.5.....	1	3.3	0.54	0.35
0.5.....	2	3.1	0.54	0.35
0.5.....	3	3.1	0.62	0.35
0.5.....	1	4.7	0.78	1.35
0.5.....	2	3.4	0.87	1.35
0.5.....	3	3.2	1.51	1.35
0.5.....	1	6.0	1.06	2.35
0.5.....	2	3.8	1.54	2.35
0.5.....	3	3.0	2.51	2.35
2.0.....	1	4.3	0.73	1.35
2.0.....	2	3.4	0.73	1.35
2.0.....	3	3.4	0.79	1.35
2.0.....	1	5.8	0.94	2.35
2.0.....	2	4.3	1.01	2.35
2.0.....	3	4.0	1.32	2.35
2.0.....	4	3.6	1.79	2.35

NOTES.— τ is the *e*-folding time for the star-formation rate, and *x* is the exponent of the power-law initial mass function. The stellar library used in these models was that of Jacoby, Hunter, and Christian 1984 and hence represents a solar neighborhood population.

ment and age, than to the rate of star formation. Table 8 gives H β and Mg *b* line strengths for various evolutionary models.

A similar comparison can be made also using color indices, but the sensitivity of the indices to the various parameters is reduced. Table 9 gives the synthetic *B*–*V* and *V*–*R* color indices, which, again, closely match the observations. The important observation to note is that the evolutionary pictures formed from the line strengths and the color indices are in accordance.

No model with an IMF exponent less than one (of any age) is able to fit the observations to within 1 σ . Even with an Salpeter exponent (*x* = 1.35), the observations, in comparison with the evolutionary models, are suggestive of a composite population (1–2 Gyr population plus an older, \sim 5 Gyr, population). A population older than 5 Gyr is possible, but optical observations such as ours do not have sufficient sensitivity to distinguish anything older. Observations such as *V*–*K* or those in the ultraviolet would help constrain the possibilities.

TABLE 9
SYNTHETIC COLOR INDICES

τ (Gyr)	Age (Gyr)	<i>B</i> – <i>V</i>	(<i>V</i> – <i>R</i>) _{KC}
A. Salpeter IMF			
0.25.....	1	0.29	0.45
0.50.....	1	0.24	0.48
0.50.....	3	0.37	0.65
0.75.....	1	0.22	0.49
0.75.....	3	0.18	0.53
0.75.....	4	0.47	0.72
0.75.....	5	0.65	0.78
1.0.....	1	0.21	0.49
1.0.....	6	0.59	0.75
B. Miller-Scalo IMF			
1.0.....	1.0	0.42	0.57
5.0.....	1.0	0.42	0.60
5.0.....	5.0	0.46	0.70
5.0.....	10.0	0.59	0.75
100.0.....	1.0	0.42	0.60
100.0.....	5.0	0.41	0.68
100.0.....	10.0	0.46	0.70
100.0.....	15.0	0.50	0.72

NOTES.—See § VI of Hamilton 1985 for an explanation of the models. Stellar library used was that of Gunn and Stryker 1983 and therefore represents a solar neighborhood population.

V. IONIZED GAS CONTENT

We observe emission-line material outside the compact nucleus, in two regimes which correspond to the narrow-line region (NLR) and disk gas. Their observed properties are listed in Table 10. We examine these properties and their implications for physical conditions, in turn.

a) The Extended Narrow-Line Region

The NLR is quite weak, with only 1% of the broad-line H α flux (assuming spherical symmetry on the sky). It is also of extremely low ionization compared to the NLRs of, for example, class 1.5 Seyfert nuclei (Cohen 1983) since no narrow [O III] emission can be identified even on our high-dispersion nuclear spectrum or in the data presented by Boksenberg *et al.* (1977). Also present is [O II] λ 3727 emission, although weak

TABLE 10
PROPERTIES OF THE EMISSION-LINE REGIONS IN THE DISK

Identification ^a	Position	[N II] λ 6583 H α	[O I] λ 6300 H α	[S II] λ 6716, 6731 H α	H α SB(mean) (ergs cm ⁻² s ⁻¹ arcsec ⁻² Å ⁻¹)	Velocity (obs)	Blue Excess	Remarks
.....	3"–8" S	1.00	...	0.3	7.7 (–17)	12526 \pm 50	Weak	NLR
.....	4"–7" N	1.22	0.1	...	7.6 (–17)	12520 \pm 50	Yes	NLR
F.....	4" S; 5" EW	1.33	0.1	0.25	5.2 (–18)	12474 \pm 50	Weak	Horseshoe
C.....	4" S; 7"–19" W	1.77	...	0.3	1.8 (–18)	12699 \pm 100	Yes	Plateau
I.....	2"7 W; 3" N–S	1.47	<0.2	...	9.7 (–18)	12583 \pm 50	Strong	
.....	5" W	1.78	...	0.4	3.7 (–18)	12668 \pm 75	No	
H.....	2"7 W; 14"–19" S	0.44	<0.1	0.3	4.3 (–18)	12317 \pm 40	No	H II
E.....	10"–15" S	0.45	<0.1	0.2	1.4 (–17)	13329 \pm 100	No	H II
B.....	5" SE–5" NW	1.01	<0.2	\sim 0.5	NLR ^b

NOTES.—Errors in v_{obs} from the internal agreement of H α , [N II] measurements. Classification of H II region-like spectra based upon results of Baldwin, Phillips, and Terlevich 1981.

^a Identification refers to the particular spectrum of Fig. 4 and to a particular spatial part as indicated in Fig. 3.

^b From high dispersion.

(Phillips 1978). Most noteworthy is the low $[\text{S II}]$ density ($\lambda 6716/\lambda 6731 = 1.71$, the low-density limit), quite unlike the values $\sim 900 \text{ cm}^{-3}$ quoted by Cohen (1983). The ionization level difference is likely due to dust close around the nucleus absorbing most of the ionizing radiation (as discussed below for disk gas), but the electron density is quite low for any kind of galactic nucleus.

The spatial extent of the NLR is also of interest. We observed peaked distribution of $[\text{N II}]$ and $\text{H}\alpha$ across $9''$ (Fig. 7), which projects to 10 kpc for $H_0 = 50 \text{ km s}^{-1} \text{ Mpc}^{-1}$. Since the bright part of the galaxy subtends only ~ 3 times this size, a substantial part of the galaxy includes gas responding to the nucleus. In fact, it is not obvious that a clear distinction is to be drawn between NLR and disk emission. The line ratios are similar (Table 10), and the spatial scales are continuous. The NLR has very narrow lines ($\text{FWHM} = 120 \text{ km s}^{-1}$), again most unusual for a Seyfert galaxy.

The IPCS spectrum in the horseshoe region reveals double $[\text{O III}] \lambda 5007$ emission with one line at 5210.0 \AA (corresponding to $v_{\text{obs}} = 12,160 \pm 200 \text{ km s}^{-1}$) and an equivalent width of 1.35 \AA . The other line is at an observed wavelength of 5217.5 \AA ($v_{\text{obs}} = 12,610 \pm 300 \text{ km s}^{-1}$) and has an equivalent width of 0.65 \AA . The lower redshift $[\text{O III}] \lambda 5007$ emission is located in a single, concentrated area on the west side of the horseshoe and has identifiable 4959 \AA emission

associated with it. The higher velocity emission is distributed across the horseshoe region.

Although none of our spectroscopic observations are blueward of 4000 \AA , from the nuclear spectrum of Bokseberg *et al.* (1977) weak $[\text{O II}] \lambda 3727$ is present also in two distinct emission features. The v_{obs} of these two lines are $11,900$ and $12,700 \text{ km s}^{-1}$. The velocity differences between the $[\text{O II}]$ and $[\text{O III}]$ are equal to within the errors. Whether or not these two sets of lines have the same (exact) radial velocities, both do show evidence of mass outflow. The best estimate of the velocity of the central system would be that derived from emission lines far out into the disk which is $12,900 \pm 100 \text{ km s}^{-1}$.

b) Emission in the Galactic Disk

The peculiar line ratios and continuity in intensity imply that the very extended emission-line material seen throughout the galaxy is related to that in the NLR, closer to the nucleus. From the line ratios alone, it appears that mechanisms other than photoionization by OB stars are responsible for producing the emission lines. The high $[\text{N II}] \lambda 6583/\text{H}\alpha$ ratio in itself insures this. Two plausible ionizing mechanisms remain, both interesting in probing conditions outside the nucleus of the galaxy associated with Mrk 231: photoionization by UV radiation from the nucleus, filtering through its thick cocoon of dust, or shocks propagating through the interstellar medium at

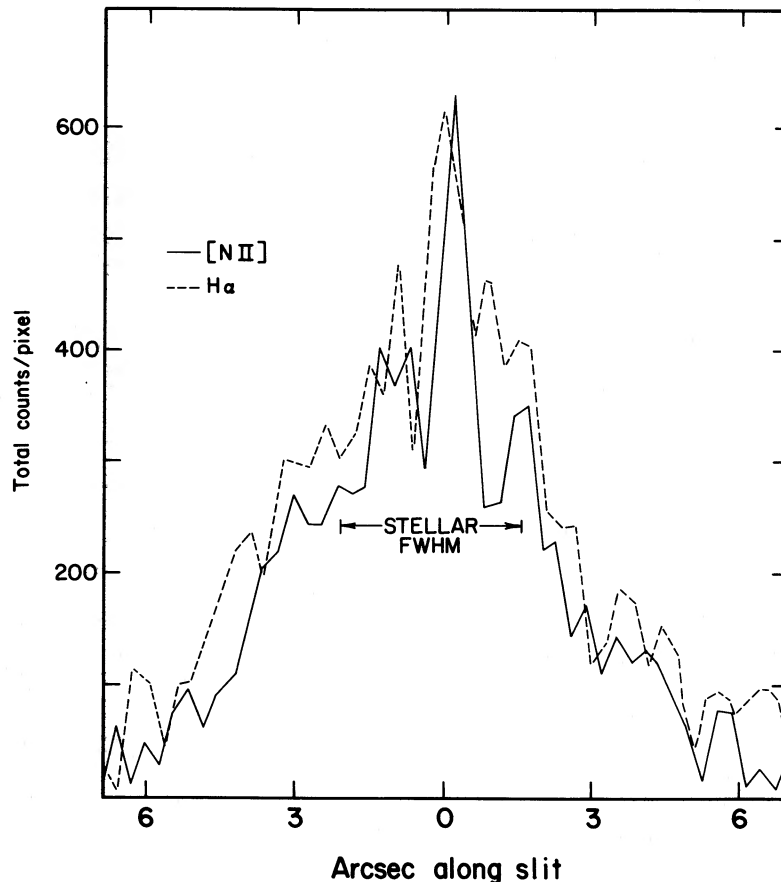


FIG. 7.—Relative intensities of $\text{H}\alpha$ and $[\text{N II}]$ across the nucleus. The FWHM points for a stellar image are marked to demonstrate the spatial extent of the emission.

$\sim 80 \text{ km s}^{-1}$. Since both processes might be present, we may set an upper limit to the effects of each by assuming all the observed emission arises from it alone.

Consider first the effects of residual nuclear radiation on the gas to the disk. In cases when large amounts of dust are not interposed, such a luminous AGN can raise the ISM of a whole galaxy to a high state of ionization, as seen in, for example, 3C 120 (Baldwin *et al.* 1980). We may set a limit on the strength of the ionizing continuum since the emission-line ratios produced by low-intensity power-law spectra are well known (Ferland and Netzer 1983; Kent and Sargent 1979; Binette 1985). By far, the dominant parameter in determining the emission-line ratios to be produced is the ionization parameter U , defined as the ratio of ionizing photon density to particle density in the emitting region. When extinction intervenes, we may write:

$$U = \frac{L_{\text{ion}} e^{-\tau}}{4\pi d^2 Nch\langle\nu\rangle} \quad (1)$$

for gas of particle number density N at a distance d from a source of L_{ion} Lyman continuum radiation per second. An effective optical depth τ and mean frequency $\langle\nu\rangle$ are used, in which the weightings due to spectral shape and extinction, respectively, are incorporated. A further ν^{-3} weighting in $\langle\nu\rangle$ is incorporated due to the photoionization cross section falloff of hydrogen immediately above the Lyman limit. A lower limit to τ may be set from the fact that the $[\text{N II}]/\text{H}\alpha$ ratio, and limit on $[\text{O III}]\lambda 5007/\text{H}\alpha$, imply that U is in the range 10^{-3} – 10^{-4} (following Ferland and Netzer 1983).

If the galaxy is flattened and nearly face-on, our westside spectrum samples a region from 5 to 15 kpc in distance from the nucleus. No density measure this far out is available (the $[\text{S II}]$ lines are too weak for a significant result), but in view of the low limit close to the nucleus, a density less than 100 cm^{-3} will be assumed. The value of L_{ion} is more difficult to derive because our own line of sight passes through considerable absorption near the nucleus. Following Boksenberg *et al.* (1977), we take the continuum to be a reddened $F_\nu = \text{constant}$ spectrum, presumably due to a quasi-thermal component of the type discussed by Malkan (1983) superposed on an underlying steeper power law. Evaluation of such a power law is normally possible using infrared measurements, but the composite infrared continuum of Mrk 231 (with a strong thermal contribution) renders this process highly uncertain. The overall 2–20 μm spectrum is close to a power law (McAlary, McLaren, and Crabtree 1979) but strong 10 μm silicate absorption suggests that a large part of the emission comes from dust heated by distributed sources (Rieke 1976), presumably the hot stellar population identified spectroscopically (Boksenberg *et al.* 1977). Rieke also notes that his data could be fitted by a model of dust distributed about the nucleus; in any case, an underlying power law cannot be extracted from available data. As extreme cases we consider $F_\nu = \text{constant}$ from the optical to the He II $\lambda 228$ ionization edge, and also extrapolate the $F_\nu \approx \nu^{-2.5}$ actually observed in the optical; the latter is an estimate of the emergent UV flux along our line of sight. Variability (Hamilton and Keel 1987) indicates that most of the optical continuum arises in the central source rather than in surrounding stars, so we use the full observed flux in these calculations without correction for starlight contamination.

These assumptions about continuum shape lead to values for ionizing flux (between 228 and 912 Å) for $4 \times 10^{-9} \text{ ergs s}^{-1} \text{ cm}^{-2}$ for $F_\nu = \text{constant}$ (using the flux scale of and correction

for the reddening $A_V = 2.3$ derived by Boksenberg *et al.* 1977) and $3 \times 10^{-12} \text{ ergs s}^{-1} \text{ cm}^{-2}$ for the $\nu^{-2.5}$ continuum (which shape includes reddening effects). For $U = 10^{-3.5}$, a density $n_e < 100$ in the disk gas implies an ionizing flux (observed at our distance) of $4.2 \times 10^{-11} \text{ ergs s}^{-1} \text{ cm}^{-2}$ or less. The comparison in terms of fluxes at the Earth is made so as to be explicitly distance (scale) independent, relying only on the angular scale of the region observed and the assumption that it lies near the plane of the sky. This indicates that the gas in the galaxy sees a continuum much more like that observed at the Earth than a normal AGN spectrum. Thus our line of sight to the nucleus is rather typical; there can be relatively few “holes” in the dust around the nucleus that allow UV radiation to escape. The solid-angle covering factor of the material producing the strong reddening is then quite close to unity. Our line of sight is typical, and by inference the extraordinary absorption-line clouds may be more isotropically distributed than required by models in which this is a typical nucleus viewed along an unusual line of sight.

This conclusion is even stronger if photoionization does not produce all of the observed emission lines. It is also of interest to consider the properties of shocked gas that might produce the emission. Using the Shull and McKee (1979) solar abundance models, the ionization constrains the typical shock velocity to be less than $\sim 85 \text{ km s}^{-1}$; this is a reasonable estimate of the highest velocities present over significant areas, since the emissivity rises rapidly with velocity and the fastest shocks will dominate the integrated spectrum. The covering factor (ratio of mean H α surface brightness to that of a single face-on shock of the same apparent size of the galaxy) is of order 0.5 for shock velocities in this range (80–90 km s^{-1}). The volume filling factor of radiating matter is, however, quite low, of order 10^{-6} for typical temperature 10^4 K .

Direct evidence for such shocks may come from high-resolution profiles of the emission lines well away from the nucleus, in which shocks might produce “turbulent broadening” well beyond that found in galactic disks. Local line widths closer to the nucleus, in the NLR, are $\sim 120 \text{ km s}^{-1}$ FWHM, from the data presented here; if such widths persist out further into the galaxy, shocks appear inevitable. Lower velocity shocks could be probed through observation of the H $_2$ feature at 2.1 μm , which is strong in gas shocked with velocities below $\sim 40 \text{ km s}^{-1}$. Tests for shocks in the ISM of Mrk 231 are especially important in view of the possibility of star formation biased to low masses, since star formation might be expected to be occurring in a very turbulent medium in which shock waves can drive cloud fragmentation to lower masses than normally present. Based on statistical trends, extremely sharp bursts of star formation with subsequent residual star formation, violates common notions regarding strong interactions.

c) Evidence for Gas Outflow

The $[\text{N II}] + \text{H}\alpha$ blend was examined in our low-dispersion spectra by fitting multiple Gaussians to the combined line profiles. Comparison of the fits and observed profiles show that an additional feature is present at several positions. As shown in Figure 8, this takes the form of excess flux on the blue side of $[\text{N II}]\lambda 6548$. This most likely represents $\text{H}\alpha$ or $\text{H}\alpha + [\text{N II}]$ at blueshifts up to 1500 km s^{-1} with respect to the galaxy.³ A similar feature has been reported in parts of NGC 4319

³ The blue excess feature is not an artifact of the Cryogenic Camera since neither arc lamp nor strong night-sky lines show the same behavior.

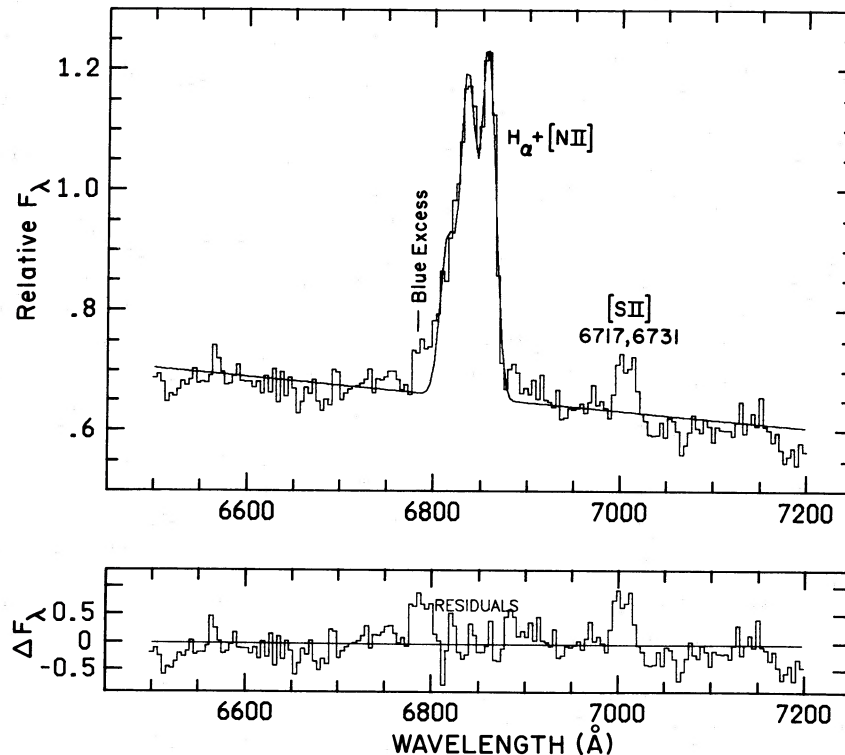


FIG. 8.—Spectrum around the region of $H\alpha$. Note the strength of $[N II]$ relative to $H\alpha$. A blue excess feature is evident from the residuals of the Gaussian fits to the $H\alpha + [N II]$ blends. This feature may be due to emission from the same lines, but at a slightly lower redshift. Both $[O II] \lambda 3727$ and $[O III] \lambda 5007$ show a double structure.

(Sulentic 1986). We tentatively interpret this as evidence for outflow, toward us (there might be similar redshifted material on the other side of the galaxy, probably hidden by dust with the system).

The spatial distribution of the “blue excess” (positions given in Table 10) shows a strong extension to the west—it is seen more than $5''$ away west, but is not seen in any other direction past $4''$, and there weakly. Thus, the flow seems to be directed to an angle toward the line of sight. This is reminiscent of the flows studied by Phillips *et al.* (1983); Wilson, Baldwin, and Ulvestad (1985); Morris *et al.* (1985); and Wilson and Baldwin (1986) in more nearby Seyfert galaxies. It is at least suggestive that the greatest apparent extent of the outflowing material roughly coincides with the direction of the extended radio structure (Ulvestad, Wilson, and Sramek 1981). If significant, this correspondence would be a unique association of wide- and narrow-angle ejection of matter from an active nucleus.

VI. DISCUSSION

a) Star Formation in Mrk 231

From a study of the region well away from the nucleus, we have found the stellar population throughout the galaxy to be rather young. The presence of a similar population close to the nucleus was inferred by Adams (1972) and Boksenberg *et al.* (1977) from the presence of high-order Balmer absorption lines (“System III”), which might be due to starlight or an intervening dense cloud. We find excellent agreement between the System III velocity of $12,900 \text{ km s}^{-1}$ (Boksenberg *et al.* 1977) and the stellar velocities off the nucleus, within 100 km s^{-1} . This lends weight to the inference that the System III absorp-

tion does in fact represent a similarly young population near the nucleus.

The strength of the young populations found from absorption lines and $H II$ emission compared to any old population component implies that the system is in (or has passed through) a kind of “slow burst” phase. The cause of such an event, and whether it bears any relation to the strong nuclear activity, is the root question here, whose answer remains obscure. Some (necessarily speculative) schemes for inducing such widespread star formation include a merger, the sudden onset of shocks or other triggers emanating from the nucleus, or the acquisition of a large amount of gas from an intergalactic cloud or gas-rich compansion. Based on the meager evidence available, we favor a merger picture for several reasons.

First, the evidence for mergers as seminal events in galaxy evolution is convincing (see, e.g., Schweizer 1986), while our other two suggestions have little grounding in hard data. Second, a strong interaction might well contribute to fueling of the active nucleus, as shown by studies encompassing a wide luminosity range among AGNs (Hutchings and Campbell 1983; Keel *et al.* 1985; Dahari 1985). Finally, we see the sort of tidal tails seen $\sim 0.5 \text{ Gyr}$ after a very close approach (Fig. 5). The amorphous nature of the disk of Mrk 231 is reminiscent of that shown by some mergers in progress (e.g., Schweizer 1982).

b) Comparison with Other Luminous Active Nuclei

The nucleus and disk of Mrk 231 are both of very high luminosity. Interesting comparisons may be drawn with other luminous AGNs whose host galaxies have been observed in

some detail. That of 3C 48 (Boroson and Oke 1982) is perhaps most similar, showing high-order Balmer absorption and integrated spectral type near A; this system has also undergone relatively recent, widespread star formation, which must have changed the galaxy luminosity and integrated spectrum substantially. If the two systems 3C 48 and Mrk 231 represent the same physical and geometrical configuration, then the distinction between them is due to the extensive dust shroud present in the latter object.

In fact, the resemblance is enhanced upon consideration of the far-infrared data from *IRAS* (Neugebauer, Soifer, and Miley 1985). They find 3C 48 and Mrk 231 to be extreme in their far-infrared excesses, and interpret the 3C 48 data as implying substantial star formation on a kiloparsec scale around the nucleus, while more of the excess in Mrk 231 is associated with the nucleus itself (from comparisons of *IRAS* 12–25 μm flux densities with small aperture measures by Rieke (1976) so separation of an extended infrared component is not feasible. We have demonstrated optically the presence of substantial numbers of young stars in the surrounding galaxy in this case as well.

There is evidence for recent star formation in several other systems with very active nuclei. The one position observed in 3C 120 by Baldwin *et al.* (1980) in which starlight was detected showed a composite, fairly early spectral type. The integrated spectrum of 3C 459 (Miller 1981) shows a weak 4000 \AA break, weak old population features, and high-order Balmer absorption, again suggesting a burst of star formation superposed over an old, normal galactic population. Heckman *et al.* (1987) have found evidence of tidal features around 3C 459. It is not yet clear, however, that the star bursts in the systems necessarily have any connection to the nuclear activity. Much remains to be done in this direction, both in probing such a connection statistically, in large numbers of host galaxies, and in examining physical processes in individual objects, as we have begun to do here.

Finally, we feel compelled to comment on the possible relationship between the blueshifted emission-line material we have observed and the prominent absorption-line systems. Both observations indicate ejection of material at high velo-

cities, 1000–6000 km s^{-1} . It is tempting to associate the emission-line material with an aged deceleration flow of the kind containing the absorption-line clouds. Further, high-resolution mapping of the optical emission will be of great interest.

VII. CONCLUSIONS

We have detected young stars and emission-line gas throughout the galaxy surrounding Mrk 231. Star formation is proceeding actively at a few positions, and has either ceased recently or has a truncated IMF in most of the galaxy. Combined with morphological information, this suggests the aftermath of a galaxy merger. The emission lines from most of the system indicate shocks or a weak power-law continuum as the ionizing agents. The line strengths imply that the nucleus is strongly obscured on all lines of sight, not just that directly observed. A narrow-line region is detected within ~ 10 kpc of the nucleus; it is of very low density and ionization, as well as large size, compared to other Seyfert galaxy nuclei. This gas merges continuously into the “disk” gas further from the nucleus.

Blue excess emission appears on the $\text{H}\alpha + [\text{N II}] \lambda\lambda 6548, 6583$ blend over a large, asymmetric area. This may be interpreted as high-velocity (1000–2000 km s^{-1}) outflow directed roughly toward us. This material might have an origin related to that of the very high-velocity absorption-line systems that are the most distinguishing features of the nucleus of Mrk 231.

We are grateful to George Will and William Binkert for assistance at the telescope. Rien de Grijp and Marijn Franx provided valuable assistance with software at Leiden. One of us (D. H.) would like to thank Wieslau Wiśniewski for assistance with the Mount Lemmon observations and reductions and to Professor H. van der Laan for the hospitality of the Sterrewacht during his two visits to Leiden. We would also like to thank Shirley Phipps and Elisa Bauer for typing of the original manuscript, to the Kitt Peak Photolab for their expert drafting and photography, and to Richard Green and Jay Gallagher for a critical reading of an early draft. The Isaac Newton Telescope is operated by the Royal Greenwich Observatory on the island of La Palma.

APPENDIX

THE NUCLEAR SPECTRUM

We can add only little to the discussion by Boksenberg *et al.* (1977) regarding the properties of the nuclear spectrum. Our spectrum of the nucleus (Fig. 4a) covers the approximate range of 4600–9200 \AA . The red data $\lambda > 7000$ \AA of Boksenberg *et al.* (1977) are from the Multichannel Spectrophotometer, and consequently it is of low spectral resolution (40 \AA vs. our 15 \AA).

One feature noted by Boksenberg *et al.* (1977) was the presence of the calcium triplet (8498, 8542, 8662 \AA) in emission. The bluest line of the triplet is close to O I $\lambda 8446$, and, with velocity broadened profiles, the two are heavily blended. We fitted to the blend (O I $\lambda 8446$ plus Ca triplet) an unweighted linear combination of Gaussian profiles with widths of ~ 1200 km s^{-1} . It was clear that a three-component (triplet only) Gaussian fit was unacceptable. The addition of O I 8446 was needed. Because of the severe blending it is not possible to derive believable line ratios or intensities. The spectral region about the calcium triplet feature along with the best fitting four-component model is given in Figure 9.

The appearance of the triplet plus O I blend is suggestive that the relative intensities of the calcium lines and to that of O I 8446 are similar to that found in galactic objects (Persson 1986; Herbig and Soderblom 1980; Persson and McGregor 1985). It would, therefore, seem plausible to assume that the physical and geometric configuration of the dust shell surrounding Mrk 231 is analogous to that of galactic objects, but on a much larger scale. The apparent relative intensities of the triplet indicate that the optical depth in these lines is not as shallow as it is in 1 Zw 1 (Persson 1986; Persson and McGregor 1985) but is still optically thick.

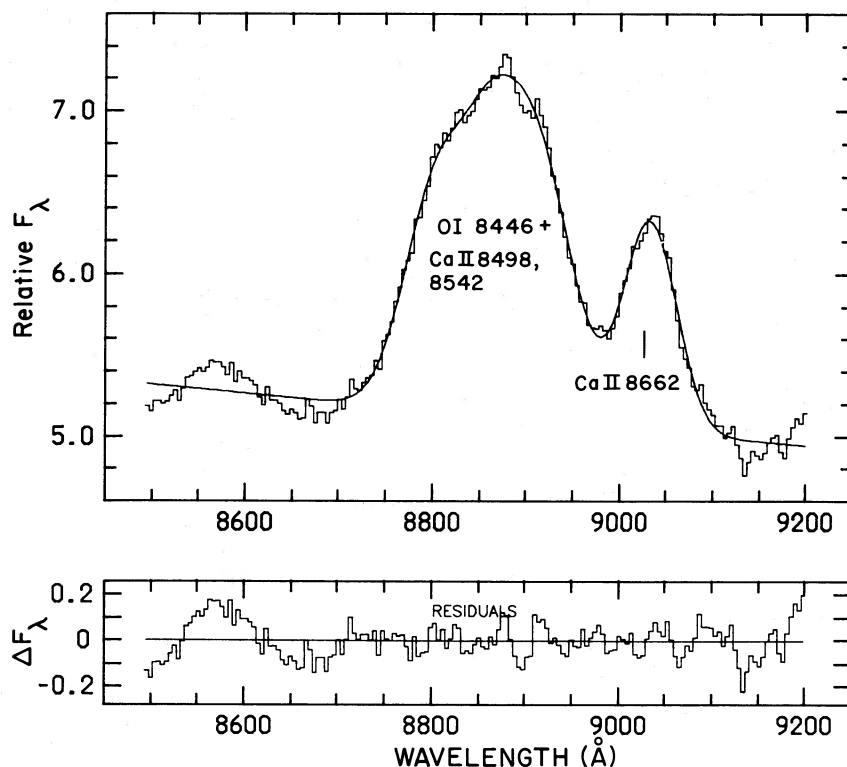


FIG. 9.—Spectrum around the calcium triplet. The continuous curve is the best fitted sum of unweighted Gaussian profiles. Note the broad emission feature at an observed wavelength of 8570 Å.

REFERENCES

- Adams, T. F. 1972, *Ap. J. (Letters)*, **176**, L1.
 ———. 1977, *Ap. J. Suppl.*, **33**, 19.
 Adams, T. F., and Weedman, D. W. 1972, *Ap. J. (Letters)* **173**, L109.
 Baldwin, J. A., Carswell, R. F., Wampler, E. J., Smith, H. E., Burbidge, E. M., and Boksenberg, A. 1980, *Ap. J.*, **236**, 388.
 Baldwin, J. A., Phillips, M., and Terlevich, R. 1981, *Pub. A.S.P.*, **93**, 5.
 Begelman, M. C. 1985, *Ap. J.*, **297**, 492.
 Binette, L. 1985, *Astr. Ap.*, **143**, 334.
 Boksenberg, A., Carswell, R. F., Allen, D. A., Fosbury, R. A. E., Penston, M. V., and Sargent, W. L. W. 1977, *M.N.R.A.S.*, **178**, 451.
 Boroson, T. A., and Oke, J. B. 1982, *Nature*, **296**, 397.
 Boroson, T. A., Persson, S. E., and Oke, J. B. 1985, *Ap. J.*, **293**, 120.
 Burbidge, E. M., and Burbidge, G. R. 1966, *Ap. J.*, **145**, 661.
 Christian, C. A., Adams, M., Barnes, J. V., Butcher, H., Hayes, D. S., Mould, J. R., and Siegel, M. 1985, *Pub. A.S.P.*, **97**, 363.
 Cohen, R. D. 1983, *Ap. J.*, **273**, 489.
 Cutri, R. M., Rieke, G. H., and Lebofsky, M. J. 1984, *Ap. J.*, **287**, 566.
 Dahari, O. 1985, *Ap. J. Suppl.*, **57**, 643.
 Ferland, G. J., and Netzer, H. 1983, *Ap. J.*, **264**, 105.
 Gunn, J. E., and Stryker, L. L. 1982, *Ap. J. Suppl.*, **52**, 121.
 Gunn, J. E., Stryker, L. L., and Tinsley, B. M. 1981, *Ap. J.*, **249**, 48.
 Hamilton, D. 1985, *Ap. J.*, **297**, 371.
 Hamilton, D., and Keel, W. C. 1987, in preparation.
 Heckman, T. M., Balick, B., and Sullivan, W. T., III. 1978, *Ap. J.*, **224**, 475.
 Heckman, T. M., Smith, E. P., Baum, S. A., van Breugel, W. J. M., Miley, G. K., Illingworth, G. D., Bothun, G. D., and Bulok, B. 1987, *A.J.*, in press.
 Herbig, G., and Soderblom, D. 1980, *Ap. J.*, **242**, 628.
 Hutchings, J. B., and Campbell, B. 1983, *Nature*, **303**, 584.
 Hutchings, J. B., Crampton, D., Campbell, B., Duncan, D., and Glendenning, B. 1984, *Ap. J. Suppl.*, **55**, 319.
 Jacoby, G., Hunter, D., and Christian, C. 1984, *Ap. J. Suppl.*, **56**, 257.
 Keel, W. C. 1983, *Ap. J.*, **269**, 466.
 ———. 1987, in preparation.
 Keel, W. C., Kennicutt, R. C., Jr., Hummel, E., and van der Hulst, J. M. 1985, *A.J.*, **90**, 708.
 Kennicutt, R. C., Jr. 1983, *Ap. J.*, **272**, 54.
 Kent, S. M., and Sargent, W. L. W. 1979, *Ap. J.*, **230**, 607.
 Malkan, M. A. 1983, *Ap. J.*, **268**, 582.
 McAlary, C. W., McLaren, R. A., and Crabtree, D. R. 1979, *Ap. J.*, **234**, 471.
 McCall, M. L., Rybski, P. M., and Shields, G. A. 1985, *Ap. J. Suppl.*, **57**, 1.
 McCutcheon, W. H., and Gregory, P. C. 1978, *Ap. J.*, **83**, 567.
 Miller, J. S. 1981, *Pub. A.S.P.*, **93**, 681.
 Morris, S., Ward, M., Whittle, M., William, A. S., and Taylor, K. 1985, *M.N.R.A.S.*, **216**, 193.
 Neugebauer, G., Soifer, B. T., and Miley, G. K. 1985, *Ap. J. (Letters)*, **295**, L27.
 Oke, J. B., and Gunn, J. G. 1983, *Ap. J.*, **266**, 713.
 Persson, S. E. 1986, *Canadian J. Phys.*, **64**, 421.
 Persson, S. E., and McGregor, P. 1985, *Ap. J.*, **290**, 125.
 Phillips, M. M. 1978, *Ap. J.*, **226**, 187.
 Phillips, M. M., Turtle, A. J., Edmunds, M. G., and Pagel, B. E. J. 1983, *M.N.R.A.S.*, **203**, 759.
 Rieke, G. H. 1976, *Ap. J. (Letters)*, **210**, L5.
 Rieke, G. H., and Low, F. J. 1972, *Ap. J. (Letters)*, **176**, L95.
 Rudy, R. J., Foltz, C. B., and Stocke, J. T. 1975, *Ap. J.*, **288**, 531.
 Sanders, D. B., Scoville, N. Z., Soifer, B. T., Young, J. S., Schloerb, F. P., Rice, W. L., Danielsen, G. S., and Persson, S. E. 1987, in *Star Formation in Galaxies*, ed. C. J. Lonsdale, in press.
 Schweizer, F. 1978, in *IAU Symposium 77, Structure and properties of Nearby Galaxies*, ed. E. M. Berkhuysen (Dordrecht: Reidel), p. 279.
 ———. 1982, *Ap. J.*, **252**, 455.
 ———. 1986, *Science*, **231**, 227.
 Shull, J. M., and McKee, C. F. 1979, *Ap. J.*, **227**, 131.
 Sulentic, J. 1986, *IAU Symposium 121, Observational Evidences of Activity of Galaxies*, ed. K. Fricke and G. Melnick (Dordrecht: Reidel), in press.
 Tyson, T. T., Baum, W. A., and Kreidl, T. 1982, *Ap. J. (Letters)*, **257**, L1.
 Ulvestad, J. S., Wilson, A. S., and Sramek, R. A. 1981, *Ap. J.*, **247**, 419.
 Weedman, D. 1971, *Ap. J.*, **183**, 29.
 White, S. D. M. 1978, *M.N.R.A.S.*, **184**, 185.
 Wilson, A. S., Baldwin, J. A., and Ulvestad, J. S. 1985, *Ap. J.*, **291**, 629.
 Wilson, A. S., and Baldwin, J. A. 1986, *Ap. J. (Letters)*, **302**, 627.

DONALD HAMILTON: National Optical Astronomy Observatories, P.O. Box 26732, Tucson, AZ 85726-6732

W. C. KEEL: Sterrewacht Leiden, Postbus 9513, 2300 RA Leiden, Nederland